


Title	Taphonomic experiments resolve controls on the preservation of melanosomes and keratinous tissues in feathers
Authors	Slater, Tiffany S.;McNamara, Maria E.;Orr, Patrick J.;Foley, Tara B.;Ito, Shosuke;Wakamatsu, Kazumasa
Publication date	2019-09-19
Original Citation	Slater, T. S., McNamara, M. E., Orr, P. J., Foley, T. B., Ito, S. and Wakamatsu, K. 'Taphonomic experiments resolve controls on the preservation of melanosomes and keratinous tissues in feathers', Palaeontology, [In press]. DOI: 10.1111/pala.12445
Type of publication	Article (peer-reviewed)
Link to publisher's version	<a href="https://onlinelibrary.wiley.com/doi/full/10.1111/pala.12445#">https://onlinelibrary.wiley.com/doi/full/10.1111/pala.12445#</a> - 10.1111/pala.12445
Rights	©The Authors. Palaeontology published by John Wiley & Sons Ltd on behalf of The Palaeontological Association This is an open access article under the terms of the Creative Commons Attribution#NonCommercial#NoDerivs License, which permits use and distribution in any medium, provided the original work is properly cited, the use is non#commercial and no modifications or adaptations are made. - <a href="http://creativecommons.org/licenses/by-nc-nd/4.0/">http://creativecommons.org/licenses/by-nc-nd/4.0/</a>
Download date	2023-05-04 20:15:36
Item downloaded from	<a href="http://hdl.handle.net/10468/8814">http://hdl.handle.net/10468/8814</a>



## TAPHONOMIC EXPERIMENTS RESOLVE CONTROLS ON THE PRESERVATION OF MELANOSOMES AND KERATINOUS TISSUES IN FEATHERS

by TIFFANY S. SLATER<sup>1</sup> , MARIA E. McNAMARA<sup>1</sup>, PATRICK J. ORR<sup>2</sup>,  
TARA B. FOLEY<sup>3</sup>, SHOSUKE ITO<sup>4</sup> and KAZUMASA WAKAMATSU<sup>4</sup>

<sup>1</sup>School of Biological, Earth & Environmental Sciences, University College Cork, Cork, Ireland; tiffany.slater@ucc.ie, maria.mcnamara@ucc.ie

<sup>2</sup>UCD, School of Earth Sciences, University College Dublin, Dublin, Ireland; patrick.orr@ucd.ie

<sup>3</sup>Department of Anatomy & Neuroscience, University College Cork, Cork, Ireland; t.foley@ucc.ie

<sup>4</sup>Department of Chemistry, Fujita Health University School of Health Sciences, Toyoake, Aichi Japan; sito@fujita-hu.ac.jp, kwaka@fujita-hu.ac.jp

Typescript received 4 February 2019; accepted in revised form 15 May 2019

**Abstract:** Fossils are a key source of data on the evolution of feather structure and function through deep time, but their ability to resolve macroevolutionary questions is compromised by an incomplete understanding of their taphonomy. Critically, the relative preservation potential of two key feather components, melanosomes and keratinous tissue, is not fully resolved. Recent studies suggesting that melanosomes are preferentially preserved conflict with observations that melanosomes preserve in fossil feathers as external moulds in an organic matrix. To date, there is no model to explain the latter mode of melanosome preservation. We addressed these issues by degrading feathers in systematic taphonomic experiments incorporating decay, maturation

and oxidation in isolation and combination. Our results reveal that the production of mouldic melanosomes requires interactions with an oxidant and is most likely to occur prior to substantial maturation. This constrains the taphonomic conditions under which melanosomes are likely to be fossilized. Critically, our experiments also confirm that keratinous feather structures have a higher preservation potential than melanosomes under a range of diagenetic conditions, supporting hitherto controversial hypotheses that fossil feathers can retain degraded keratinous structures.

**Key words:** mouldic melanosome, fossil colour, fossil feather, experimental taphonomy, melanin, keratin.

Fossil feathers play a pivotal role in our understanding of the evolutionary processes underlying the transition from non-avian dinosaurs to birds. Feathers comprise primarily melanosomes embedded in a keratinous matrix, both of which have been the subject of extensive research (Schweitzer *et al.* 1999a; Vinther *et al.* 2008; McNamara *et al.* 2013; Moyer *et al.* 2016; Pan *et al.* 2016, 2019) in both modern and palaeontological contexts in order to understand better the underlying drivers in the evolution of feathers and flight. Keratin is a fibrous protein rich in cysteine, which promotes extensive cross-linking (and thus confers chemical stability) via disulfide bonds (Wang *et al.* 2016). Keratinous tissues can be preserved in fossils by replacement in authigenic minerals (Briggs *et al.* 1997; Benton *et al.* 2008; Manning *et al.* 2009; McNamara *et al.* 2018a). Reports of organically preserved keratinous tissues (Schweitzer *et al.* 1999a; Moyer *et al.* 2016; Pan *et al.* 2016, 2019), however, are disputed (Saitta *et al.* 2017a, b). The other key component of many (but not all) feathers are melanosomes, micron-sized organelles rich in melanin pigments that occur in two primary forms: eumelanin, a

heterogenous polymer derived from oxidation of the amino acid tyrosine (Solano 2014) and pheomelanin, derived from tyrosine and sulfur-rich L-cysteine (Ito & Wakamatsu 2008). Melanosomes and chemical evidence for melanin have been reported from soft tissues associated with many exceptionally preserved fossils (Vinther *et al.* 2008; Wogelius *et al.* 2011; Barden *et al.* 2015; Lindgren *et al.* 2015). Such discoveries have stimulated attempts to reconstruct the original colouration of fossil birds, reptiles and avian and non-avian dinosaurs (Li *et al.* 2010; Zhang *et al.* 2010; Lindgren *et al.* 2014, 2017; McNamara *et al.* 2016a; Vinther *et al.* 2016; Hu *et al.* 2018) and have provided insights into palaeoecology (Brown *et al.* 2017; Smithwick *et al.* 2017) and the evolution of communication strategies (McNamara *et al.* 2016a; Lindgren *et al.* 2017).

Despite such extensive research, the taphonomy of melanin and melanosomes is incompletely understood. Chemical evidence for preservation of the melanin molecule has been reported from fossil fish eyes (Lindgren *et al.* 2012), reptile skin (Lindgren *et al.* 2014), frog internal tissues (McNamara *et al.* 2018b) and cephalopod ink

sacs (Glass *et al.* 2012). This, plus the preservation of melanosomes, has been attributed to the inherent resistance of melanin to alteration (Glass *et al.* 2012) by enzymatic digestion (Ohtaki & Seiji 1971) and acid hydrolysis (Borovanský *et al.* 1977). Recent work, however, demonstrates that diagenetic processes can impact the chemistry of melanosomes, e.g. the incorporation of sulfur (sulfurization) can promote preservation (McNamara *et al.* 2016b); conversely, certain processes, especially oxidation, can degrade melanin (Korytowski & Sarna 1990).

Little is known about the physical taphonomy of melanosomes. Experiments have demonstrated that maturation of melanosomes results in diagenetic shrinkage (McNamara *et al.* 2013). Paradoxically, despite the inherent recalcitrance of melanosomes, many fossil feathers display extensive regions where melanosomes are preserved as external moulds; the melanosomes themselves are degraded (Li *et al.* 2010, figs 1c–g, 2a–b, e–f; Zhang *et al.* 2010, figs 1b–c, 2b–e, 3b, 4b–d; Lindgren *et al.* 2015, supplementary figs 2a–h, 3a–e). The physical and chemical conditions under which this occurs are unknown, and hypotheses relating to the nature of the diagenetic processes responsible (Vinther 2015, 2016) remain untested. The chemistry of the mould-bearing matrix is particularly controversial. Previous studies have speculated that mouldic melanosomes are embedded in the degraded remains of the originally keratinous matrix (Zhang *et al.* 2010), but this hypothesis is not universally accepted (Saitta *et al.* 2017a, b); rather, the matrix surrounding some fossil melanosomes has been interpreted as sediment infill following keratin decay (Saitta *et al.* 2017b). Moulds in fossil feathers have been interpreted as sites formerly occupied by decay bacteria (Moyer *et al.* 2014), but the taphonomic mechanism responsible is unknown.

Here, we address these issues by experimentally degrading feathers from extant birds in controlled laboratory experiments. We analysed feather microstructure using SEM and TEM and feather chemistry using alkaline hydrogen peroxide oxidation (AHPO) followed by high-performance liquid chromatography (HPLC). Our results reveal the taphonomic pathways that favour preservation of melanosomes and keratinous feather components and the conditions under which melanosome degradation can produce moulds in a keratinous matrix.

## MATERIAL AND METHOD

### *Justification for experimental design*

Decay and maturation were integrated in our experiments as both processes impact preservation (Briggs 2003). For experiments using temperature only, samples were placed in Al foil packets; samples for experiments combining

temperature and pressure were placed within Au capsules. It has been proposed that maturation of tissues in Al foil packets may result in the potential loss of labile and recalcitrant materials (Saitta *et al.* 2019). While loss of volatiles (gases and water) may occur in this scenario, previous experiments demonstrate that more recalcitrant materials (including melanosomes and the surrounding keratinous matrix) can survive maturation (McNamara *et al.* 2013). One criticism of maturation in sealed Au capsules is that these may prevent loss of labile materials (Saitta *et al.* 2019). In natural systems, however, confining sediment may prevent at least localized loss of labile materials from tissues.

The optimum experimental conditions are those that are geologically realistic and that generate the phenomena or processes being investigated. Our goal was to investigate the controls on melanosome degradation in feathers that retain recognizable branching structure after experimentation, as in the fossils of interest. We therefore used similar experimental conditions to those of McNamara *et al.* (2013), which are known to retain gross feather structure and melanosomes. Conditions using higher temperature and pressure (such as those used in Saitta *et al.* 2017a, b) do not preserve recognizable feather structure.

### *Simulated taphonomic pathways*

Taphonomic experiments simulated a suite of pathways (1–16; Table 1) under oxic conditions using the following variables: decay, pH, oxidation, temperature and pressure (Fig. 1; Slater *et al.* 2019, fig. S1). Untreated feathers were used as a control. Pathways 1–7 test individual variables. Pathways 8–11 test various combinations of decay (at pH 6), oxidation and maturation, where oxidation precedes maturation (where used). These collectively comprise taphonomic sequence 1 (Table 1; Slater *et al.* 2019, fig. S1). Taphonomic sequence 2 is based on maturation prior to, or simultaneous with, oxidation and incorporates pathways 12–16 (Table 1; Slater *et al.* 2019, fig. S1).

### *Material*

Black contour feathers from the uropygial region of the zebra finch, *Taeniopygia guttata* (n = 3) were stored at –80°C prior to treatment via pathways 1–16. Black primary feathers from *Gallus gallus* (common chicken, n = 3) were used for AHPO analysis due to the large sample size required (individual specimens of *T. guttata* yielded insufficient black regions from tail feathers); feather samples from this taxon were treated to pathways 5, 8, 12 and 13. For all experiments, three replicate feather samples (one from each of three specimens) of similar colour (as assessed visually) were used. Replicate

**TABLE 1.** Experimental setup showing taphonomic sequences, experimental conditions used and natural scenarios corresponding to experimental pathways.

Pathway	Decay		Oxidation		Maturation		Natural analogue
	pH 6	pH 12.2	Occurrence	Timing	Without pressure	With pressure	
Control							—
1	X						Decay in slightly acidic sediments/pore waters
2		X					Decay in highly alkaline fluids
3					X		Thermal maturation
4						X	High temperature-high pressure maturation
5			X				Oxidation by pore fluids
6	X				X		Decay followed by high temperature maturation
7	X					X	Decay followed by high temperature-high pressure maturation
Sequence 1							
8	X		X				Decay followed by oxidation by pore fluids
9	X		X	Before maturation	X		Decay followed by oxidation by pore fluids and then by high temperature maturation
10			X	Before maturation	X		Oxidation by pore fluids followed by high temperature maturation
11			X	Before maturation		X	Oxidation by pore fluids followed by high temperature-high pressure maturation
Sequence 2							
12	X		X	After maturation	X		Decay followed by high temperature maturation and then by oxidation by pore fluids upon exhumation
13			X	After maturation	X		Thermal maturation followed by oxidation by pore fluids upon exhumation
14	X		X	After maturation		X	Decay followed by high temperature-high pressure maturation and then by oxidation by pore fluids upon exhumation
15			X	After maturation		X	High temperature-high pressure maturation followed by oxidation by pore fluids upon exhumation
16			X	Simultaneous with maturation	X		Oxidation by pore fluids and thermal maturation occur simultaneously

*G. gallus* samples for individual pathways were combined for AHPO analyses.

#### Decay experiments

Feathers were placed in sterile glass vials containing 5 ml distilled deionized water with no added inoculum. Decay experiments in pathways 1, 6–9, 12 and 14 used a starting pH of 6.0. Decay experiments in pathway 2 used a starting pH of 12.2; pH was adjusted via the addition of  $K_2CO_3$ . Pathway 2 tested in isolation the impact of the elevated pH used in the oxidation experiment. Vials were sealed loosely with aluminium foil, covered by parafilm and placed in a Memmert constant temperature incubator for 1 month at  $30 \pm 1^\circ C$ . Decayed feathers were stored in 70% ethanol prior to analysis.

#### Maturation experiments

Feathers were experimentally matured using one of two approaches: (1) high temperature; and (2) high temperature combined with high pressure. (1) Feathers were placed in Al foil and matured in a standard laboratory convection oven at  $200 \pm 1^\circ C$  for 1 h. (2) Feathers were placed in Au tubes and matured in a customized Strata-Tech water-pressurized cold-seal autoclave at  $200^\circ C$ , 135 bar for 1 h.

#### Oxidation experiments

Degradation of melanosomes in a laboratory context is difficult. Lysosomal digestion (Ohtaki & Seiji 1971) removes melanosomal proteins but does not alter the

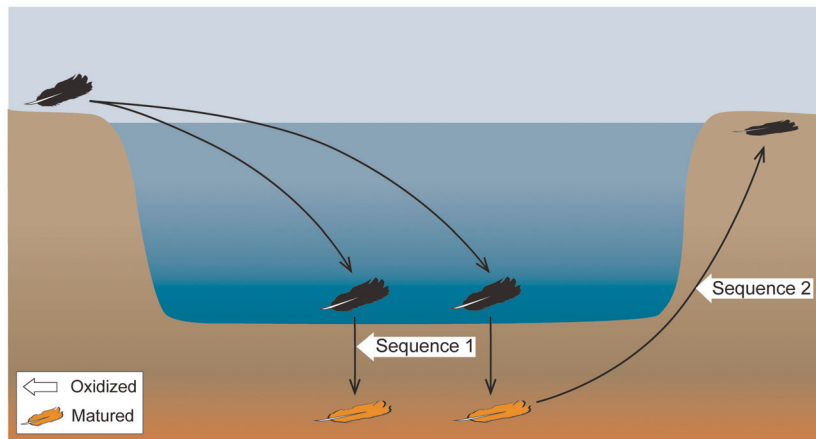


**FIG. 1.** Experimental sequences. Schematic showing potential natural scenarios incorporating experimental pathways 8–16. Sequence 1 is based on oxidation prior to maturation (where used); sequence 2 is based on oxidation following maturation. Experiments included some, or all, of decay, maturation and oxidation (with various parameters used for decay and maturation; for details see Table 1 and Slater *et al.* 2019, fig. S1).

melanin molecule; acid hydrolysis decarboxylates melanin (Ito *et al.* 2018) but does not alter melanosome geometry (Borovanský *et al.* 1977). The only treatment known to degrade melanosomes in a laboratory context is oxidation in a highly alkaline solution, which ruptures the melanosomal membrane and solubilizes melanin (Smith *et al.* 2017). Feather samples were oxidized using a modified version of the AHPO protocol described in Ito *et al.* (2011). Samples (0.5–1 mg) were placed in an Eppendorf tube to which 100 µl DD water, 375 µl 1 M K<sub>2</sub>CO<sub>3</sub> and 25 µl 30% H<sub>2</sub>O<sub>2</sub> were added to produce a final concentration of 1.5% H<sub>2</sub>O<sub>2</sub> at a pH of 12.2. The tubes were agitated at 175 rpm for 20 h, and the experiment stopped by adding 50 µl 10% Na<sub>2</sub>SO<sub>3</sub> and 140 µl of 6 M HCl. The tubes were centrifuged for 1 min at 5500 rpm and samples placed in an ultrasonic bath with DD water for 15–30 s to remove precipitates. Experiments for pathway 16 (synchronous oxidation and high temperature maturation) were carried out at 150°C until the solution fully evaporated (30 min) without addition of Na<sub>2</sub>SO<sub>3</sub> and HCl as in other experiments using oxidation.

#### AHPO

AHPO is a chemical assay that allows identification and quantification of melanin via diagnostic chemical markers that are derived from the 5,6-dihydroxyindole (DHI) parent subunits of the melanin molecule. The markers for eumelanin are pyrrole-2,3,5-tricarboxylic acid (PTCA), pyrrole-2,3-dicarboxylic acid (PDCA) and pyrrole-2,3,4,5-tetracarboxylic acid (PTECA); PTCA is a marker for the 5,6-dihydroxyindole-2-carboxylic acid (DHICA) unit with a carboxyl group attached at the 2-position of DHI (Ito

*et al.* 2011); PDCA is a marker for the dihydroxyindole unit (DHI); and PTECA is a marker for thermally altered (cross-linked) DHI units and is thus used as a marker for eumelanin in fossils (Glass *et al.* 2012; McNamara *et al.* 2018b). Feather samples (4 mg) treated as per experimental pathways 5, 8, 12 and 13, and aliquots (100 µl) of the oxidizing solution were analysed via HPLC as follows. Feather tissue (4 mg) from each pathway was homogenized in distilled water with a Ten-Broeck glass homogenizer at a concentration of 10 mg/ml. Aliquots (100 µl) of this and the oxidizing solution were then subjected to AHPO (Ito *et al.* 2011).

#### SEM

Small (2–3 mm<sup>2</sup>) fragments of barbs were dissected using sterile tools, dehydrated and embedded in LR White resin using standard protocols (Pan *et al.* 2016). Resin blocks were cut using a Leica EM UC7 ultramicrotome with a 45° diamond knife and mounted on Al stubs with carbon tape. Blocks were then sputter coated with Au/Pd and analysed using an FEI Inspect SEM at an accelerating voltage of 10 kV and working distance of 8 mm. Where melanosomes could not be readily observed (e.g. on the surface of the resin block), barbs were fractured and mounted on carbon conductive tape on Al stubs.

#### TEM

Ultrathin (80 nm) sections were placed on Cu grids. Sections were stained with 3% uranyl acetate (5 min) and 0.3% lead citrate (2 min) using standard protocols (Lewis & Knight 1977) and examined using a JEOL 2000FXII transmission electron microscope at 80 kV.



### Statistical analysis

Quantitative data on the abundance of mouldic melanosomes was collected from transverse sections through barbules as follows. The number of moulds was calculated per unit area for untreated samples and for samples that were treated with oxidation (pathways 8–15). Differences in the number of moulds between samples were assessed using an unpaired *t*-test.

## RESULTS

### Generation of mouldic melanosomes

Three-dimensional micron-sized moulds are apparent in many of the experimentally treated feathers (Figs 2E, 3, 4C, 5C). Similar features reported previously in decay experiments were interpreted as moulds of decay bacteria

by Moyer *et al.* (2014). The moulds generated in our experiments are not of decay bacteria as they: (1) are visible in feathers that were not decayed; (2) occur only internally within the feather cortex; and (3) no bacteria were observed on decayed feather surfaces. Further, the geometry of the moulds produced in our experiments is consistent with that of melanosomes in transverse sections of feathers (Slater *et al.* 2019, table S1). The structures we observed are thus clearly mouldic melanosomes; this is supported by our chemical data, which confirm the presence of melanin markers in the experimental media (see below).

SEM images show that the feather barb cortex contains densely packed melanosomes. In all of our experiments moulds are less abundant per unit area than are the melanosomes, suggesting that not all melanosomes were degraded. The relative abundance of moulds, however, varies among experimental treatments; these variations are discussed below.

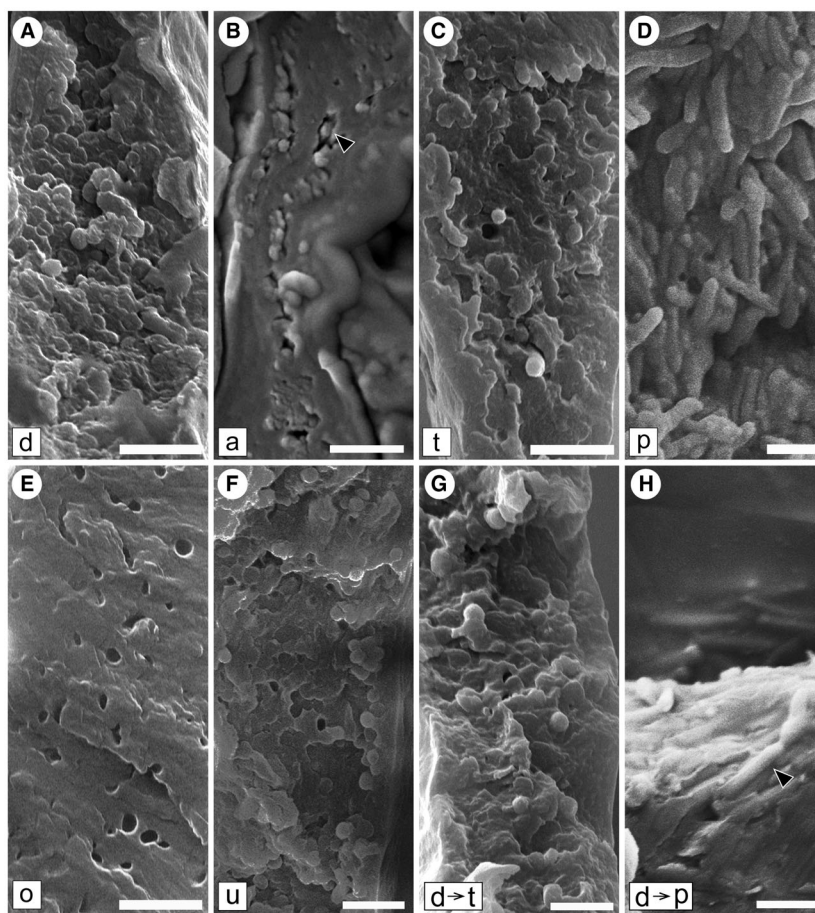


**FIG. 2.** SEM images of feather barbules. A, pathway 1. B, pathway 2. C, pathway 3. D, pathway 4. E, pathway 5. F, untreated. G, pathway 6. H, pathway 7. A, C, F–H, transverse fractured surfaces. B, D, E, transverse microtomed surfaces. a, decay at pH 12.2; d, decay at pH 6; o, oxidized; p, matured with pressure; t, matured without pressure; u, untreated; black arrowheads, 3D melanosomes. All scale bars represent 1  $\mu$ m.

### Pathways 1–7

Moulds are absent in all samples prepared from untreated feathers and pathways 1–4, 6 and 7 (Table 1; Figs 2A–D, F–H, 4A–B, 5A–B). The presence of moulds in feathers from pathway 5 is thus not an artefact of preparation (Fig. 2E). It is also consistent with the variation seen in the experimental data (see below). Some distortion of the shape of the moulds is difficult to prevent when sectioning such material for TEM (as opposed to imaging SEM samples; see Fig. 4C).

### Taphonomic sequence 1

Abundant moulds were generated via pathways 8–11 (0.55, 1.23, 1.53 and 1.03 moulds/ $\mu\text{m}^2$ , respectively; Figs 3A–D, 4C, 5C). In TEM images, feathers from pathway 8 exhibit moulds and few intact melanosomes (Fig. 4C; feathers from pathways 9–11 were not analysed using TEM). Maturation did not destroy moulds generated during a previous oxidation step (pathways 9, 10 and 11; Fig. 3B–D).

### Taphonomic sequence 2

Mouldic melanosomes are absent or rare in feathers degraded via pathways 12–15 (0.05, 0.52, 0.31 and 0.01 moulds/ $\mu\text{m}^2$ , respectively; Figs 3E–H, 4D). Three-dimensional melanosomes, however, are abundant (Figs 3G–H, 4D). Feathers treated via pathway 16 were degraded to a translucent residue that lacked obvious barbs and barbules (Fig. 5D); melanosomes and moulds could not be identified.

### Abundance of mouldic melanosomes and melanin concentrations

Fewer moulds were produced in taphonomic sequence 2 ( $0.22 \pm 0.24$  moulds/ $\mu\text{m}^2$ ) than sequence 1 ( $1.09 \pm 0.41$  moulds/ $\mu\text{m}^2$ ; these differences are statistically significant ( $t$ -test result:  $t(6) = 3.62$ ,  $p = 0.01$ ). We analysed feather samples and experimental media from pathways 5, 8, 12 and 13 using AHPO. All feathers analysed contain lower concentrations of the eumelanin markers PTCA ( $244.4 \pm 91.8$  ng/mg) and PTeCA ( $106.4 \pm 27.6$  ng/mg) than the corresponding experimental media ( $1313.2 \pm 420$  and  $349.9 \pm 169$  ng/mg, respectively) (Fig. 6); these differences are statistically significant ( $t(14) = 3.08$ ,  $p = 0.008$ ). Higher quantities of eumelanin markers are present in the experimental media from treatments lacking maturation (pathways 5 and 8) relative to treatments including a

maturation step (pathways 12 and 13). Feathers treated to decay and oxidation only (pathway 8), and their experimental media, contain higher concentrations of eumelanin markers than in any other experimental treatment; further, media from these and other decayed samples (i.e. pathway 12) show higher PTeCA/PTCA ratios than non-decayed feathers (pathways 5 and 13; Slater *et al.* 2019, table S3). The significant differences in the abundance of both melanin and melanosomes between feathers treated via sequences 1 and 2 strongly suggest that our data reflect real experimentally-induced differences and not original variations in melanin content (McGraw *et al.* 2005) among the individual feathers analysed.

## DISCUSSION

Sample preparation was consistent for each treatment and so relative differences in the abundance of moulds among samples are almost certainly real and not artefacts. Compressed moulds in ultrathin sections from pathway 8 (Fig. 4C) are an artefact of microtomy and may reflect enhanced susceptibility of the feather to mechanical damage during sectioning due to experimental treatment (Fig. 5C).

### Controls on melanosome preservation

The restriction of moulds to oxidized feathers (Figs 2–4) strongly suggests that interaction with an oxidant is prerequisite to the formation of mouldic melanosomes in fossils. Decay does not result in the production of mouldic melanosomes, even under alkaline conditions (which are known to enhance melanin solubility; Figs 2, 4) (Wakamatsu *et al.* 2012). The lower concentrations of eumelanin markers in feathers relative to experimental media (Fig. 6) demonstrate that all treatments analysed using AHPO resulted in loss of melanin from feathers. Nevertheless, the presence of melanin markers in all experimentally-treated feathers analysed provides robust experimental evidence that fossil feathers with diverse taphonomic histories have the potential to retain melanin and/or its diagnostic alteration products. This supports the hypothesis that the melanin identified in fossil feathers derives from melanosomes and not decay bacteria (*contra* Moyer *et al.* 2014).

The preservation of abundant moulds following maturation (including maturation at high pressure) in pathways 9–11 confirms that moulds that form early during the diagenetic process can survive subsequent thermal alteration and elevated pressures. Preservation of mouldic melanosomes does not, therefore, imply little or no maturation during burial.

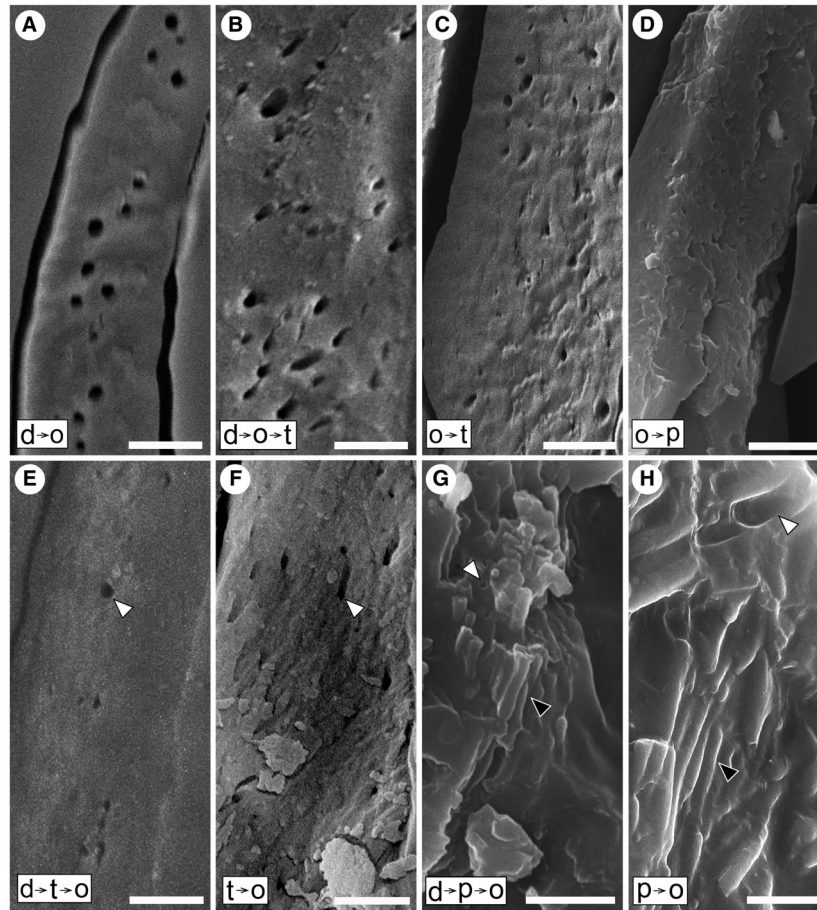


**FIG. 3.** SEM images of feather barbules. A, pathway 8. B, pathway 9. C, pathway 10. D, pathway 11. E, pathway 12. F, pathway 13. G, pathway 14. H, pathway 15. A–C, E–F, transverse microtomed surfaces. D, G–H, transverse fractured surfaces. d, decay at pH 6; o, oxidized; p, matured with pressure; t, matured without pressure; black arrowheads, 3D melanosomes; white arrowheads, mouldic melanosomes. All scale bars represent 1  $\mu$ m.

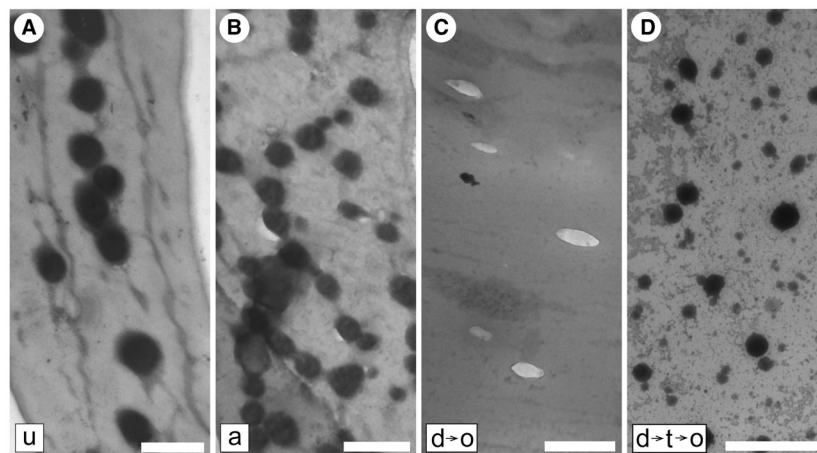


**FIG. 4.** TEM images of feather barbules. A, untreated. B, pathway 2. C, pathway 8. D, pathway 12. Melanosomes appear black; moulds appear as light-toned ovoids. a, decay in alkaline conditions (pH 12.2); d, decay at pH 6; o, oxidized; t, matured without pressure; u, untreated. All scale bars represent 500 nm.



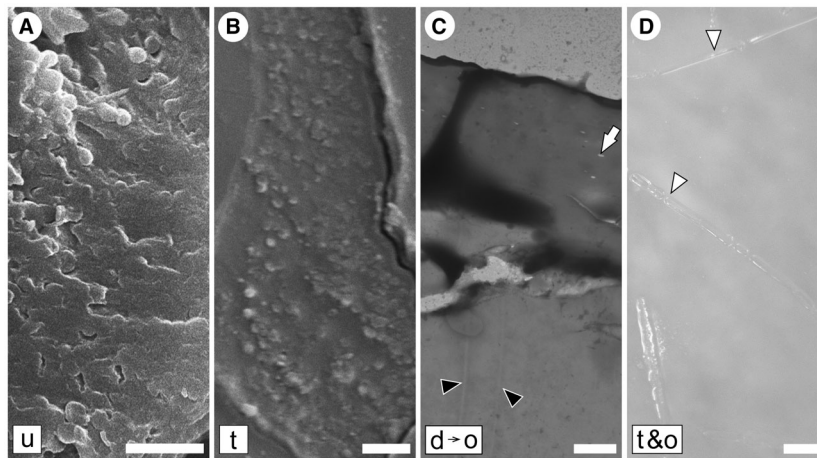


**FIG. 5.** Additional features of experimentally treated feathers. A–B, SEM images of transverse microtomed surfaces in untreated feathers (A) and feathers from pathway 3 (B). C, TEM image of feather barbule from pathway 8 (see Fig. 4C for additional examples of compressed voids at higher resolution). D, light micrograph of feather barbs following experimental treatment in pathway 16. d, decayed; o, oxidized; t, matured without pressure; u, untreated; black arrowheads, blade marks showing direction of cutting during microtomy; white arrow, compressed moulds; white arrowheads, translucent barbs. All scale bars represent 1  $\mu\text{m}$  except D (1 mm).

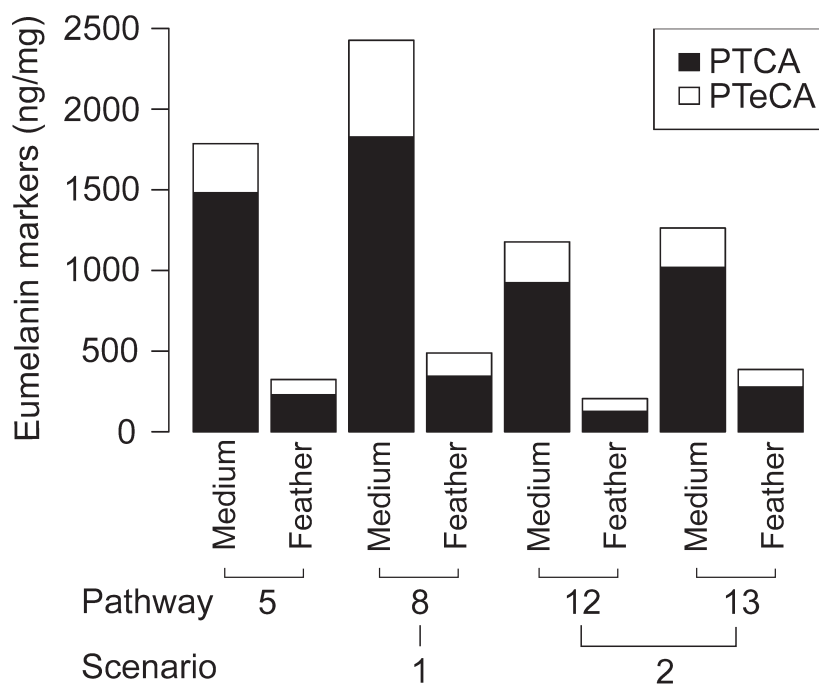


**FIG. 6.** AHPO analysis of *Gallus gallus* feathers and their experimental media. PTCA and PTeCA are eumelanin markers (PTeCA is a marker for diagenetically altered melanin).

Published images of fossil feathers typically show broad regions where adjacent melanosomes are preserved predominantly either as moulds or as intact microbodies (Li *et al.* 2010, figs 1c–g, 2a–b, e–f; Zhang *et al.* 2010, figs 1b–c, 2b–e, 3b, 4b–d; Lindgren *et al.* 2015, supplementary figs 2a–h, 3a–e). This contrasts with our results from pathways 12–15, which show that oxidation after

maturation with pressure results in a heterogeneous distribution (at a micron-scale) of intact and mouldic melanosomes and overall fewer moulds than where oxidation precedes maturation. Instead, patterns in melanosome preservation in fossils are more consistent with our results from sequence 1 and strongly suggest the presence of a taphonomic switch from a system favouring

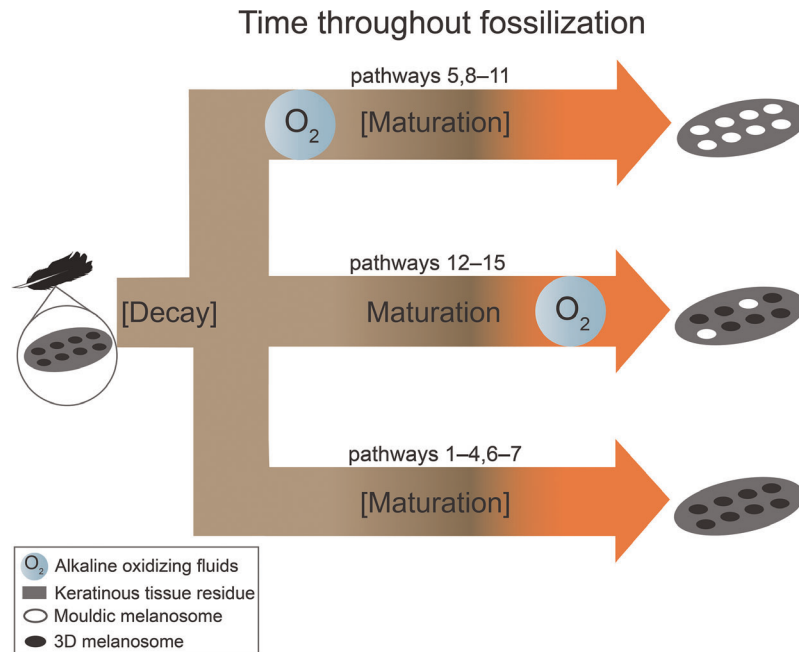


**FIG. 7.** The impact of various taphonomic conditions on melanosome preservation. Grey ovoid denotes transverse section of feather barbule. Arrows indicate time. Brackets indicate that a particular taphonomic process is not always present. Pathway 16 is not shown as it involved simultaneous exposure to an oxidant and elevated temperatures, and the presence/absence of melanosomes and moulds could not be confirmed in the degraded residue.

preservation of melanosomes as 3D bodies to one favouring preservation as moulds that is controlled by the timing of oxidant availability relative to maturation.

To date, mouldic melanosomes have been reported from Konservat-Lagerstätten that are hosted in sediments interpreted to have been deposited within oxic (Zhou *et al.* 2016) or dysoxic/anoxic bottom waters (Pedersen 1981). Various chemical species, however, can act as oxidants. Manganese-based oxidants are strongest in alkaline (Messaoudi *et al.* 2001; Dash *et al.* 2009) and oxic (Antoniou *et al.* 2014) environments and also at oxic-anoxic interfaces (Jones *et al.* 2018). Nitrates are strong oxidants under both acidic and alkaline conditions (Quin *et al.* 2015), while halogens (e.g. chlorine and fluorine) can maintain a high oxidation potential under various pH conditions when present in high quantities (Steininger & Pareja 1996). Copper is an oxidant under acidic and alkaline conditions (Celante & Freitas 2010) and is known to accelerate the oxidation of melanin via Fenton-like reactions (Korytowski & Sarna 1990).

The AHPO results provide further insights into the preservation of melanosomal melanin. The higher quantity of PTeCA in the experimental medium from pathway 8 relative to that from pathway 5 suggests that decay enhances melanosome degradation. In addition, the higher PTeCA:PTCA values for pathway 12 relative to pathway 13 indicate that melanosome oxidation may be enhanced when feathers have undergone some decay.

Despite this, the lower concentrations of eumelanin markers in treatments including both decay and maturation relative to treatments involving decay but not maturation suggest that maturation is a more important control on melanin preservation than decay (Glass *et al.* 2013). The preservational mechanism for the remnant melanosomes presumably reflects, at least in part, *in-situ* polymerization processes which are responsible for the organic preservation of various fossil tissues (McNamara *et al.* 2016b). Collectively, our experimental results suggest that feathers exposed to (an) oxidizing agent(s) prior to substantial maturation are likely to possess more mouldic melanosomes than feathers that experienced maturation prior to oxidation (Fig. 7). This does not exclude the possibility that some moulds may form following maturation; further, if feathers experience decay following exposure to strong oxidizing agents, it is possible that moulds may be occluded by collapse of the feather. Our experiments show that the primary controls on melanosome and melanin preservation are (in decreasing order of importance): exposure to an oxidant, the extent of maturation, and decay.

#### Keratin preservation

The survival of feather residues in the fossil record (Zhang *et al.* 2010; Pan *et al.* 2016, 2019) is controversial

(Saitta *et al.* 2017a, b). Chemical evidence of keratin has been reported from various Mesozoic and Cenozoic fossils (Schweitzer *et al.* 1999a, b; Edwards *et al.* 2011; Pan *et al.* 2016, 2019) and organic matrices surrounding fossil feather melanosomes have been interpreted as degraded residues of originally keratinous feather tissue (Li *et al.* 2010; Zhang *et al.* 2010; Gren *et al.* 2017) or diagenetic replacements thereof (Lindgren *et al.* 2015). These findings have been disputed on the basis of recent taphonomic experiments on feathers (Saitta *et al.* 2017a–b, 2019). Maturation experiments on black feathers in Au cells for 24 h at 100°C, 250 bar resulted in the transformation of the tissue to a black pellet (Saitta *et al.* 2017b); at 250°C, 250 bar, feather structure transformed to a fluid (Saitta *et al.* 2017a). Further, Saitta *et al.* (2019) reported loss of keratinous tissues in feather barbs experimentally matured in sediment. The pellets and barb imprints were not tested for chemical evidence of keratin or its residues (Saitta *et al.* 2017b, 2019). Pyrolysis-GC-MS analyses of the fluid failed to provide unequivocal evidence for keratin (Saitta *et al.* 2017a); this, however, is not unexpected as: (1) keratin and melanin produce similar pyrolysates; and (2) it is unlikely that keratinous components would survive the elevated temperatures used in such analyses. The microstructure of fossil feathers has also been the basis of hypotheses relating to the preservation of keratinous residues. Exposure of melanosomes in fossils has been interpreted as evidence that keratin components should rarely be preserved (Saitta *et al.* 2017a). While examples of fossil feathers preserving only melanosomes certainly exist (e.g. Hu *et al.* 2018, fig. 5c), our experiments confirm that three-dimensional melanosomes and keratinous components of feathers can both persist under various taphonomic conditions. Critically, our experiments also identify a suite of taphonomic conditions where keratinous components of feathers can survive, yet melanosomes do not. These results support previous interpretations that organic matrices surrounding fossil melanosomes represent degraded residues of originally keratinous feather tissue (Li *et al.* 2010; Zhang *et al.* 2010; McNamara *et al.* 2013; Pan *et al.* 2016).

## CONCLUSIONS

Our findings suggest that organic residues preserved in some fossil feathers are ideal targets for chemical and immunohistochemical analyses for remnants of keratin. Such residues have been reported in Cretaceous fossils with primitive feather types (Li *et al.* 2010; Zhang *et al.* 2010; Lindgren *et al.* 2015); analysis of these, and older, fossils has the potential to yield important insights into feather chemistry at key stages of feather evolution. Our

investigation into the differential preservation of feather components provides a robust framework for future experiments as it allows the impact of different taphonomic factors (and their relative timing) on feather preservation to be assessed. Combination of this rigorous experimental approach with chemical analyses will provide critical empirical data to test fossil-based models for the survival of keratin and melanin in the fossil record.

**Acknowledgements.** The research was funded by European Research Council Starting Grant 2014-ERC-StG-637691-ANICO-LEVO awarded to MEM. We thank Giliane Odin, Suzanne Crotty, Vince Lodge and Joe Tobin for assistance with SEM and TEM and Jack Connell and Liam Hayes for supplying feathers. Johan Lindgren and an anonymous referee are thanked for useful comments.

**Author contributions.** TSS performed all analyses with assistance from MEM and TBF; TSS, MEM and PJO co-wrote the paper with input from all other authors; MEM and PJO conceived the study; MEM and TSS designed the research; SI and KW performed AHPO analyses.

## DATA ARCHIVING STATEMENT

Data for this study are available in the Dryad Digital Repository: <https://doi.org/10.5061/dryad.7290t40>

**Editor.** Robert Sansom

## REFERENCES

- ANTONIOU, A., BREUKELN, B. M. VAN and STUYF-ZAND, P. J. 2014. Aquifer pre-oxidation using permanganate to mitigate water quality deterioration during aquifer storage and recovery. *Applied Geochemistry*, **50**, 25–36.
- BARDEN, H. E., BERGMANN, U., EDWARDS, N. P., EGERTON, V. M., MANNING, P. L., PERRY, S., VEELEN, A. van, WOGELIUS, R. A. and DONGEN, B. E. van 2015. Bacteria or melanosomes? A geochemical analysis of micro-bodies on a tadpole from the Oligocene Enspel Formation of Germany. *Palaeobiodiversity & Palaeoenvironments*, **95**, 33–45.
- BENTON, M. J., ZHOU, Z., ORR, P. J., ZHANG, F. and KEARNS, S. L. 2008. The remarkable fossils from the Early Cretaceous Jehol Biota of China and how they have changed our knowledge of Mesozoic life: presidential address, delivered 2nd May 2008. *Proceedings of the Geologists' Association*, **119**, 209–228.
- BOROVANSKÝ, J., HACH, P. and DUCHOŇ, J. 1977. Melanosome: an unusually resistant subcellular particle. *Cell Biology International Reports*, **1**, 549–554.
- BRIGGS, D. E. G. 2003. The role of decay and mineralization in the preservation of soft-bodied fossils. *Annual Review of Earth & Planetary Sciences*, **31**, 275–301.

- WILBY, P. R., PÉREZ-MORENO, B. P., SANZ, J. L. and FREGENAL-MARTÍNEZ, M. 1997. The mineralization of dinosaur soft tissue in the Lower Cretaceous of Las Hoyas, Spain. *Journal of the Geological Society*, **154**, 587–588.
- BROWN, C. M., HENDERSON, D. M., VINTHER, J., FLETCHER, I., SISTIAGA, A., HERRERA, J. and SUMMONS, R. E. 2017. An exceptionally preserved three-dimensional armored dinosaur reveals insights into coloration and Cretaceous predator-prey dynamics. *Current Biology*, **27**, 2514.e3–2521.e3.
- CELANTE, V. G. and FREITAS, J. G. 2010. Electrodeposition of copper from spent Li-ion batteries by electrochemical quartz crystal microbalance and impedance spectroscopy techniques. *Journal of Applied Electrochemistry*, **40**, 233–239.
- DASH, S., PATEL, S. and MISHRA, B. K. 2009. Oxidation by permanganate: synthetic and mechanistic aspects. *Tetrahedron*, **65**, 707–739.
- EDWARDS, N. P., BARDEN, H. E., DONGEN, B. E. van, MANNING, P. L., LARSON, P. L., BERGMANN, U., SELLERS, W. I. and WOGELIUS, R. A. 2011. Infrared mapping resolves soft tissue preservation in 50 million year-old reptile skin. *Proceedings of the Royal Society B*, **278**, 3209–3218.
- GLASS, K., ITO, S., WILBY, P. R., SOTA, T., NAKAMURA, A., BOWERS, C. R., VINTHER, J., DUTTA, S., SUMMONS, R., BRIGGS, D. E. G., WAKAMATSU, K. and SIMON, J. D. 2012. Direct chemical evidence for eumelanin pigment from the Jurassic period. *Proceedings of the National Academy of Sciences*, **109**, 10218–10223.
- — — — — MILLER, K. E., DUTTA, S., SUMMONS, R. E., BRIGGS, D. E. G., WAKAMATSU, K. and SIMON, J. D. 2013. Impact of diagenesis and maturation on the survival of eumelanin in the fossil record. *Organic Geochemistry*, **64**, 29–37.
- GREN, J. A., SJÖVALL, P., ERIKSSON, M. E., SYLVESTERSEN, R. L., MARONE, F., SIGFRIDSSON CLAUSS, K. G. V., TAYLOR, G. J., CARLSON, S., UVDAL, P. and LINDGREN, J. 2017. Molecular and microstructural inventory of an isolated fossil bird feather from the Eocene Fur Formation of Denmark. *Palaeontology*, **60**, 73–90.
- HU, D., CLARKE, J. A., ELIASON, C. M., QIU, R., LI, Q., SHAWKEY, M. D., ZHAO, C., D'ALBA, L., JIANG, J. and XU, X. 2018. A bony-crested Jurassic dinosaur with evidence of iridescent plumage highlights complexity in early paravian evolution. *Nature Communications*, **9**, 1–12.
- ITO, S. and WAKAMATSU, K. 2008. Chemistry of mixed melanogenesis—pivotal roles of dopaquinone. *Photochemistry & Photobiology*, **84**, 582–592.
- NAKANISHI, Y., VALENZUELA, R. K., BRILLIANT, M. H., KOLBE, L. and WAKAMATSU, K. 2011. Usefulness of alkaline hydrogen peroxide oxidation to analyze eumelanin and pheomelanin in various tissue samples: application to chemical analysis of human hair melanins. *Pigment Cell & Melanoma Research*, **24**, 605–613.
- MIYAKE, S., MARUYAMA, S., SUZUKI, I., COMMO, S., NAKANISHI, Y. and WAKAMATSU, K. 2018. Acid hydrolysis reveals a low but constant level of pheomelanin in human black to brown hair. *Pigment Cell & Melanoma Research*, **31**, 393–403.
- JONES, M., NICO, P., YING, S., REGIER, T., THIEME, J. and KEILUWEIT, M. 2018. Manganese-driven carbon oxidation at oxic-anoxic interfaces. *Environmental Science & Technology*, **52**, 12349–12357.
- KORYTOWSKI, W. and SARNA, T. 1990. Bleaching of melanin pigments. Role of copper ions and hydrogen peroxide in autooxidation and photooxidation of synthetic dopa-melanin. *Journal of Biological Chemistry*, **265**, 12410–12416.
- LEWIS, P. and KNIGHT, D. 1977. Staining methods for sectioned material. In GLAUERT, A. M. (ed.). *Practical methods in electron microscopy series*. Vol. 5. North-Holland Publishing Company, Amsterdam, 547 pp.
- LI, Q., GAO, K. Q., VINTHER, J., SHAWKEY, M. D., CLARKE, J. A., D'ALBA, L., MENG, Q., BRIGGS, D. E. G. and PRUM, R. O. 2010. Plumage color patterns of an extinct dinosaur. *Science*, **327**, 1369–1372.
- LINDGREN, J., UVDAL, P., SJÖVALL, P., NILSSON, D. E., ENGDAHL, A., SCHULTZ, B. P. and THIEL, V. 2012. Molecular preservation of the pigment melanin in fossil melanosomes. *Nature Communications*, **3**, 1–7.
- SJÖVALL, P., CARNEY, R. M., UVDAL, P., GREN, J. A., DYKE, G., SCHULTZ, B. P., SHAWKEY, M. D., BARNES, K. R. and POLCYN, M. J. 2014. Skin pigmentation provides evidence of convergent melanism in extinct marine reptiles. *Nature*, **506**, 484–488.
- — — CINCOTTA, A., UVDAL, P., HUTCHESON, S. W., GUSTAFSSON, O., LEFÈVRE, U., ESCUILLIÉ, F., HEIMDAL, J., ENGDAHL, A., GREN, J. A., KEAR, B. P., WAKAMATSU, K., YANS, J. and GODEFROIT, P. 2015. Molecular composition and ultrastructure of Jurassic paravian feathers. *Scientific Reports*, **5**, 1–13.
- KURIYAMA, T., MADSEN, H., SJÖVALL, P., ZHENG, W., UVDAL, P., ENGDAHL, A., MOYER, A. E., GREN, J. A., KAMEZAKI, N., UENO, S. and SCHWEITZER, M. H. 2017. Biochemistry and adaptive colouration of an exceptionally preserved juvenile fossil sea turtle. *Scientific Reports*, **7**, 13324.
- MANNING, P. L., MORRIS, P. M., McMAHON, A., JONES, E., GIZE, A., MACQUAKER, J. H. S., WOLFF, G., THOMPSON, A., MARSHALL, J. and TAYLOR, K. G. 2009. Mineralized soft-tissue structure and chemistry in a mummified hadrosaur from the Hell Creek Formation, North Dakota (USA). *Proceedings of the Royal Society B*, **276**, 3429–3437.
- McGRAW, K. J., SAFRAN, R. J. and WAKAMATSU, K. 2005. How feather colour reflects its melanin content. *Functional Ecology*, **19**, 816–821.
- McNAMARA, M. E., BRIGGS, D. E. G., ORR, P. J., FIELD, D. J. and WANG, Z. 2013. Experimental maturation of feathers: implications for reconstructions of fossil feather colour. *Biology Letters*, **9**, 1–6.
- ORR, P. J., KEARNS, S. L., ALCALÁ, L., ANADÓN, P. and PEÑALVER, E. 2016a. Reconstructing carotenoid-based and structural coloration in fossil skin. *Current Biology*, **26**, 1075–1082.



- DONGEN, B. E. van, LOCKYER, N. P., BULL, I. D. and ORR, P. J. 2016b. Fossilization of melanosomes via sulfurization. *Palaeontology*, **59**, 337–350.
- ZHANG, F., KEARNS, S. L., ORR, P. J., TOULOUSE, A., FOLEY, T., HONE, D. W. E., ROGERS, C. S., BENTON, M. J., JOHNSON, D. and XU, X. 2018a. Fossilized skin reveals coevolution with feathers and metabolism in feathered dinosaurs and early birds. *Nature Communications*, **9**, 1–7.
- KAYE, J. S., BENTON, M. J., ORR, P. J., ROSSI, V., ITO, S. and WAKAMATSU, K. 2018b. Non-integumentary melanosomes can bias reconstructions of the colours of fossil vertebrates. *Nature Communications*, **9**, 1–9.
- MESSAOUDI, B., JOIRET, S., KEDDAM, M. and TAKENOUTI, H. 2001. Anodic behaviour of manganese in alkaline medium. *Electrochimica Acta*, **46**, 2487–2498.
- MOYER, A. E., ZHENG, W., JOHNSON, E. A., LAMANNA, M. C., LI, D.-Q., LACOVARA, K. J. and SCHWEITZER, M. H. 2014. Melanosomes or microbes: testing an alternative hypothesis for the origin of microbodies in fossil feathers. *Scientific Reports*, **4**, 1–9.
- — and SCHWEITZER, M. 2016. Keratin durability has implications for the fossil record: results from a 10 year feather degradation experiment. *PLoS One*, **11**, e0157699.
- OHTAKI, N. and SEIJI, M. 1971. Degradation of melanosomes by lysosomes. *Journal of Investigative Dermatology*, **57**, 1–5.
- PAN, Y., ZHENG, W., MOYER, A. E., O'CONNOR, J. K., WANG, M., ZHENG, X., WANG, X., SCHROETER, E. R., ZHOU, Z. and SCHWEITZER, M. H. 2016. Molecular evidence of keratin and melanosomes in feathers of the Early Cretaceous bird *Eoconfuciusornis*. *Proceedings of the National Academy of Sciences*, **113**, E7900–E7907.
- — SAWYER, R. H., PENNINGTON, M. W., ZHENG, X., WANG, X., WANG, M., HU, L., O'CONNOR, J., ZHAO, T., LI, Z., SCHROETER, E. R., WU, F., XU, X., ZHOU, Z. and SCHWEITZER, M. 2019. The molecular evolution of feathers with direct evidence from fossils. *Proceedings of the National Academy of Sciences*, **116**, 3018–3023.
- PEDERSEN, G. K. 1981. Anoxic events during sedimentation of a Palaeogene diatomite in Denmark. *Sedimentology*, **28**, 487–504.
- QUIN, P., JOSEPH, S., HUSSON, O., DONNE, S., MITCHELL, D., MUNROE, P., PHELAN, D., COWIE, A. and van ZWIETEN, L. 2015. Lowering N<sub>2</sub>O emissions from soils using eucalypt biochar: the importance of redox reactions. *Scientific Reports*, **5**, 1–14.
- SAITTA, E. T., ROGERS, C. S., BROOKER, R. A., ABBOTT, G. D., KUMAR, S., O'REILLY, S. S., DONOHUE, P., DUTTA, S., SUMMONS, R. E. and VINTHER, J. 2017a. Low fossilization potential of keratin protein revealed by experimental taphonomy. *Palaeontology*, **60**, 547–556.
- — — and VINTHER, J. 2017b. Experimental taphonomy of keratin: a structural analysis of early taphonomic changes. *Palaios*, **32**, 647–657.
- KAYE, T. G. and VINTHER, J. 2019. Sediment-encased maturation: a novel method for simulating diagenesis in organic fossil preservation. *Palaeontology*, **62**, 135–150.
- SCHWEITZER, M. H., WATT, J. A., AVCI, R., KNAPP, L., CHIAPPE, L., NORELL, M. and MARSHALL, M. 1999a. Beta-keratin specific immunological reactivity in feather-like structures of the Cretaceous alvarezsaurid, *Shuvuia deserti*. *Journal of Experimental Zoology*, **285**, 146–157.
- — — FORSTER, C. A., KRAUSE, D. W., KNAPP, L., ROGERS, R. R., BEECH, I. and MARSHALL, M. 1999b. Keratin immunoreactivity in the Late Cretaceous bird *Rahonavis ostromi*. *Journal of Vertebrate Paleontology*, **19**, 712–722.
- SLATER, T. S., McNAMARA, M. E., ORR, P. J., FOLEY, T. B., ITO, S. and WAKAMATSU, K. 2019. Data from: Taphonomic experiments resolve controls on the preservation of melanosomes and keratinous tissues in feathers. *Dryad Digital Repository*. <https://doi.org/10.5061/dryad.7290t40>
- SMITH, R. A. W., GARRETT, B., NAQVI, K. R., FÜLÖP, A., GODFREY, S. P., MARSH, J. M. and CHECHIK, V. 2017. Mechanistic insights into the bleaching of melanin by alkaline hydrogen peroxide. *Free Radical Biology & Medicine*, **108**, 110–117.
- SMITHWICK, F. M., NICHOLLS, R., CUTHILL, I. C. and VINTHER, J. 2017. Countershading and stripes in the theropod dinosaur *Sinosauropteryx* reveal heterogeneous habitats in the Early Cretaceous Jehol Biota. *Current Biology*, **27**, 1–7.
- SOLANO, F. 2014. Melanins: skin pigments and much more—types, structural models, biological functions, and formation routes. *New Journal of Science*, **2014**, 1–28.
- STEININGER, J. M. and PAREJA, C. 1996. ORP sensor response in chlorinated water. NSPI Water Chemistry Symposium, Phoenix. *NSPI Symposium Series*, **1**.
- VINTHER, J. 2015. A guide to the field of palaeo colour: melanin and other pigments can fossilise: reconstructing colour patterns from ancient organisms can give new insights to ecology and behaviour. *BioEssays*, **37**, 643–656.
- 2016. Fossil melanosomes or bacteria? A wealth of findings favours melanosomes. *BioEssays*, **38**, 220–225.
- BRIGGS, D. E., PRUM, R. O. and SARANATHAN, V. 2008. The colour of fossil feathers. *Biology Letters*, **4**, 522–525.
- NICHOLLS, R., LAUTENSCHLAGER, S., PITTMAN, M., KAYE, T. G., RAYFIELD, E., MAYR, G. and CUTHILL, I. C. 2016. 3D camouflage in an ornithischian dinosaur. *Current Biology*, **26**, 2456–2462.
- WAKAMATSU, K., NAKANISHI, Y., MIYAZAKI, N., KOLBE, L. and ITO, S. 2012. UVA-induced oxidative degradation of melanins: fission of indole moiety in eumelanin and conversion to benzothiazole moiety in pheomelanin. *Pigment Cell & Melanoma Research*, **25**, 434–445.
- WANG, B., YANG, W., MCKITTRICK, J. and MEYERS, M. A. 2016. Keratin: structure, mechanical properties, occurrence in biological organisms, and efforts at bioinspiration. *Progress in Materials Science*, **76**, 229–318.

- WOGELIUS, R. A., MANNING, P. L., BARDEN, H. E., EDWARDS, N. P., WEBB, S. M., SELLERS, W. I., TAYLOR, K. G., LARSON, P. L., DODSON, P. and YOU, H. 2011. Trace metals as biomarkers for eumelanin pigment in the fossil record. *Science*, **333**, 1622–1626.
- ZHANG, F., KEARNS, S. L., ORR, P. J., BENTON, M. J., ZHOU, Z., JOHNSON, D., XU, X. and WANG, X. 2010. Fossilized melanosomes and the colour of Cretaceous dinosaurs and birds. *Nature*, **463**, 1075–1078.
- ZHOU, L., ALGEO, T. J., FENG, L., ZHU, R., PAN, Y., GAO, S., ZHAO, L. and WU, Y. 2016. Relationship of pyroclastic volcanism and lake-water acidification to Jehol Biota mass mortality events (Early Cretaceous, northeastern China). *Chemical Geology*, **428**, 59–76.